Inorg. Chem. **2006**, *45*, 5145–5149

Synthesis and Characterization of Ag Nanoshells by a Facile Sacrificial Template Route through in situ Replacement Reaction

Minghai Chen and Lian Gao*

State Key Laboratory of High Performance Ceramics and Superfine Microstructure, Shanghai Institute of Ceramics, Chinese Academy of Sciences, Shanghai 200050, P. R. China

Received March 30, 2006

A facile in situ replacement reaction route was successfully introduced for synthesizing Ag nanoshells with outer diameters of 40–50 nm and inner diameters of 20–30 nm using Co nanoparticles as sacrificial templates. The products were characterized by XRD, TEM, SAED, and UV–vis absorption spectra. The formation mechanism was also discussed. The reaction driving force comes from the large reduction potential gap between the Ag^{+}/Ag and Co^{2+}/Co redox couples, which results in the consumption of Co cores and the formation of a hollow cavity of Ag nanoshells. The UV–vis spectrum of this nanostructure exhibits a distinct difference from that of solid nanoparticles, which makes it a good candidate for application in photothermal materials.

Introduction

In the past decade, the synthesis of noble metal nanostructures has been an active research area because of the importance of these materials to catalysis, photography, electronics, photonics, information storage, optoelectronics, biological labeling, imaging, and sensing.[1,2] As noble metals are reduced in size to tens of nanometers, a very strong new absorption is observed that results from the collective oscillation of the electrons in the conduction band from one surface of the particle to the other. This is called the surface plasmon resonance (SPR), which has become the focus of research work on noble metal nanostructures.[3−6] As the most important noble metal, silver's nanostructure has attracted great interest. The intrinsic properties of nanostructures can be tailored by controlling their size, shape, composition, crystallinity, and structure (e.g., solid or hollow). Great effort has been paid to control the shape of the nanostructure, and all kinds of morphologies have been successfully prepared, such as nanowires, nanorods, nanocubes, nanoplates,[1] and nanoprisms.[7,8] However, hollow nanostuctures have rarely been reported because of the difficulty in preparing them.

Metallic nanoshells are one of the most interesting and possibly useful materials of the recently developed nanostructures. Generally, most of the preparations of the noble metal nanoshell are focused on the template strategy, in which noble nanoparticles are attached to the surfaces of template spheres. The commonly used templates include silica[9] and polystyrene spheres.[10,11] But because of the large size of the present sphere, both the outer diameter and the cavity size of the obtained nanoshells are in the range of hundreds of nanometers, which limits the practical applications and the basic study. Furthermore, the removal of the core will always bring a negative effect to the nanoshell structure. It is of great importance to reduce the size to nanoscale. So, selecting a smaller sacrificial core will practically resolve this problem. Xia et al.[12−17] successfully prepared Au and Pt hollow nanostructures using a Ag

* To whom correspondence should be addressed. E-mail: liangaoc@online.sh.cn. Tel.: 0086-21-52412718. Fax: 0086-21-52413122.

(1) Wiley, B.; Sun, Y.; Mayers, B.; Xia, Y. *Chem.—Eur. J.* **2005**, *11*, 454.
(2) Tsuji, M.; Hashimoto, M.; Nishizawa, Y.; Kubokawa, M.; Tsuji, T. *Chem.—Eur. J.* **2005**, *11*, 440.
(3) Hao, E.; Li, S.; Bailey, R. C.; Zou, S.; Schatz, G. C.; Hupp, J. T. J. *Phys. Chem. B* **2004**, *108*, 1224.
(4) Baer, R.; Neuhauser, D.; Weiss, S. *Nano Lett.* **2004**, *4*, 85.
(5) Schwartzberg, A. M.; Grant, C. D.; Wolcott, A.; Talley, C. E.; Huser, T. R.; Bogomolni, R.; Zhang, J. Z. *J. Phys. Chem. B* **2004**, *108*, 19191.
(6) Zhang, J.; Li X.; Sun, X.; Li, Y. *J. Phys. Chem. B* **2005**, *109*, 12544.
(7) Sun, Y.; Mayers, B.; Xia, Y. *Nano Lett.* **2003**, *3*, 675.
(8) Jin, R.; Cao, Y.; Mirkin, C. A.; Kelly, K. L.; Schatz, G. C.; Zheng, J. G. *Science* **2001**, *294*, 1901.
(9) Lu, L.; Zhang, H.; Sun, G.; Xi, S.; Wang, H.; Li, X.; Wang, X.; Zhao, B. *Langmuir* **2003**, *19*, 9490.
(10) Pol, V. G.; Grisaru, H.; Gedanken, A. *Langmuir* **2005**, *21*, 3635.
(11) Zhang, J.; Liu, J.; Wang, S.; Zhan, P.; Wang, Z.; Ming, N. *Adv. Funct. Mater.* **2004**, *14*, 1089.
(12) Sun, Y.; Mayers, B.; Xia, Y. *Adv. Mater.* **2003**, *15*, 641.
(13) Chen, J.; Saeki, F.; Wiley, B. J.; Cang, H.; Cobb, M. J.; Li, Z. Y.; Au, L.; Zhang, H.; Kimmey, M. B.; Li, X. D.; Xia, Y. *Nano Lett.* **2005**, *5*, 473.
(14) Sun, Y.; Xia, Y. *Nano Lett.* **2003**, *3*, 1569.
(15) Sun, Y.; Mayers, B. T.; Xia, Y. *Nano Lett.* **2002**, *2*, 481.
(16) Sun, Y.; Xia, Y. *J. Am. Chem. Soc.* **2004**, *126*, 3892.

10.1021/ic060539j CCC: $33.50
Published on Web 05/18/2006

nanostructure as the sacrificial template. But how can the Ag hollow structure be prepared? It is a precondition that the core materials are more reactive than silver. Although Ni,[18] Co,[19−21] and Pb[22] nanoparticles have been reported as serving as core materials to construct an M@N (M= Ni, Co, Pb; N = Ag, Au, Pt) core−shell nanostructure, there are few successful reports on the synthesis of Ag nanoshells through this facile route. Recently, Liang et al.[23,24] successfully synthesized Au and Pt hollow nanospheres using newly prepared cobalt nanoparticles as sacrificial templates, and the SPR properties of Au nanoshells could be well-tuned by controlling the interior cavity sizes. In the present work, Ag hollow nanoshells were successfully synthesized by a similar strategy using Co nanoparticles as sacrificial templates, which were thoroughly depleted during the process. This unique hollow Ag nanostructure is expected to be used in drug delivery, biological labeling, catalysis, and high performance SPR applications.

Experimental Section

All chemicals were of analytical grade and used as received without further purification. In a typical experimental procedure, 0.038 g of citric acid and 0.06 g of $NaBH_4$ were dissolved in 200 mL of deionized water; 0.8 mL of a $Co(NO_3)_2$ solution (0.1 M) was then rapidly injected into the solution to form a brown solution (denoted as solution I). In the meantime, 1.6 mL of a $AgNO_3$ solution (0.1 M) was diluted to 50 mL (denoted as solution II). After several minutes, the bubble ceased to release from the reaction between surplus $NaBH_4$ with water in solution I. Solution II was then mixed with solution I with rapid agitation. The color of the mixture gradually changed from brown to deep green and formed a stable colloidal solution. The products were collected by centrifugation at 8000 rpm for 30 min.

Powder X-ray diffraction (XRD) was carried out in a Japan Rigaku D/max 2550V X-ray diffractometer using Cu Kα (λ = 0.15406 nm) radiation at 40 kV and 60 mA. TEM and HRTEM images were collected using a JEOL-2100F electron microscope. FE-SEM images were collected on a JSM 6700F field-emission scanning electron microscope. EDS was recorded on an OXFORD ISIS spectroscope, which was attached to the JEOL-2100F electron microscope. UV−vis absorption spectrum analysis was performed on a Shimadzu UV-3101PC spectrophotometer.

Results and Discussion

In the present work, Co nanoparticles were synthesized by the reduction of Co^{2+} by $NaBH_4$. Although the major products from this reduction reaction are always Co_2B (eq 1), metallic Co can be formed during the sacrificial oxidation/reduction reaction (eq 2).[25] Considering the whole experiment is conducted under ambient conditions, the dissolving of O_2 in the solution is inevitable and provided the required O_2 for reaction 2. The replacement reaction driving force comes from the large reduction potential gap between the Ag^+/Ag and Co^{2+}/Co redox couples. Because the reduction potential of the Ag^+/Ag (0.799 V vs SHE) redox couple is higher than that of Co^{2+}/Co (−0.377 V vs SHE), the following replacement reaction (eq 3) can occur spontaneously as soon as a Ag^+ ion contacts with metallic Co.

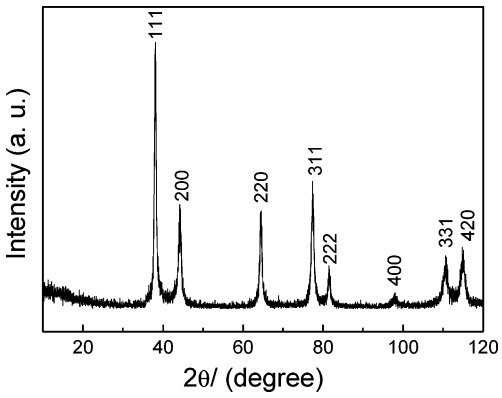

Figure 1. XRD pattern of the as-prepared Ag nanoshells

$$2Co^{2+} + 4BH_4^- + 9H_2O \rightarrow Co_2B + 12.5H_2 + 3B(OH)_3 \quad (1)$$

$$4Co_2B + 3O_2 \rightarrow 8Co + 2B_2O_3 \quad (2)$$

$$Co + 2Ag^+ \rightarrow 2Ag + Co^{2+} \quad (3)$$

The XRD pattern of the as-prepared sample is shown in Figure 1. All the diffraction peaks can be well-indexed to face-centered cubic silver with calculated lattice constants of a = 4.08 Å, which is in good agreement with the value in the literature (JCPDS card No. 04-0783, a = 4.086 Å). No impurities are detected, which shows the high purity of the product. It also confirms the high efficiency of reaction 1. The morphologies of the sample were observed by TEM and SEM, which are shown in Figure 2. In Figure 2a, the low-magnification TEM image shows the well dispersed nanoparticles with diameters of 40−50 nm. Close observation shows a strong contrast difference between the center and edge, which suggests a hollow nanostructure. The corresponding SAED rings in Figure 2b indicate the good crystallinity of the product, and all the rings can be indexed to fcc Ag. As marked in Figure 2b, the centric rings can be assigned to the (111), (200), (220), and (311) planes. The high-magnification micrograph (Figure 2c) clearly shows the hollow nanoshell, showing outer diameters of 40−50 nm and inner diameter of 20−30 nm. The FE-SEM image in Figure 2d further shows the morphology of the nanosphere. The HRTEM image of a single nanoshell is shown in Figure 3, showing the high crystallinity. The stripes spacing are measured to be 0.236 and 0.2 nm, which is close to the plane spacing of (111) and (200), respectively. As marked in Figure

(17) Sun, Y.; Wiley, B.; Li, Z. Y.; Xia, Y. *J. Am. Chem. Soc.* **2004**, *126*, 9399.
(18) Bala, T.; Bhame, S. D.; Joy, P. A.; Prasad, B. L. V.; Sastry, M. *J. Mater. Chem.* **2004**, *14*, 2941.
(19) Sobal, N. S.; Hilgendorff, M.; Mohwald, H.; Giersig, M.; Spasova, M.; Radetic, T.; Farle, M. *Nano Lett.* **2002**, *2*, 621.
(20) Sobal, N. S.; Ebels, U.; Mohwald, H.; Giersig, M. *J. Phys. Chem. B* **2003**, 107, 7351.
(21) Bala, T.; Arumugam, S. K.; Pasricha, R.; Prasad, B. L. V.; Sastry, M. *J. Mater. Chem.* **2004**, *14*, 1057.
(22) Wang, Y.; Cai, L.; Xia, Y. *Adv. Mater.* **2005**, *17*, 473.
(23) Liang, H. P.; Wan, L. J.; Bai, C. L.; Jiang, L. *J. Phys. Chem. B* **2005**, *109*, 7795.
(24) Liang, H. P.; Zhang, H. M.; Hu, J. S.; Guo, Y. G.; Wan, L. J.; Bai, C. L. *Angew. Chem., Int. Ed.* **2003**, *43*, 1540.
(25) Glavee, G. N.; Klabunde, K. J.; Sorensen, C. M.; Hadjipanayis, G. C. *Langmuir* **1993**, *9*, 162.

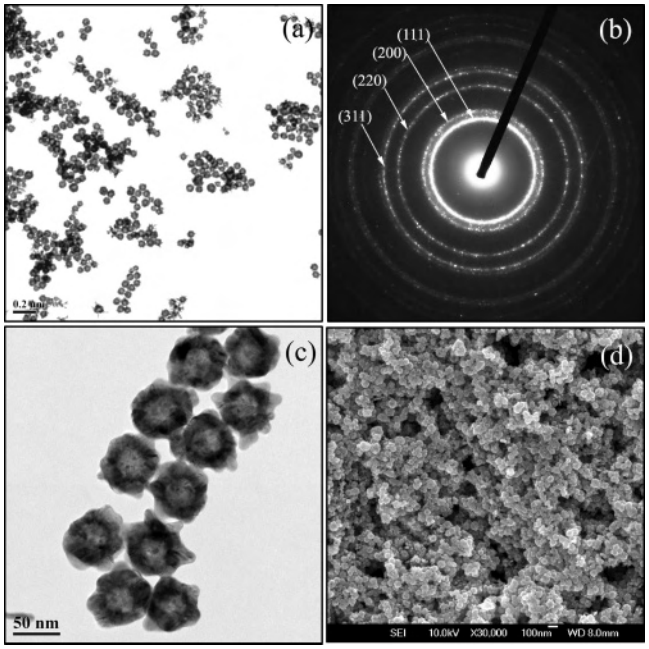

Figure 2. Morphology of the as-prepared Ag nanoshell: (a) low-magnification TEM image, (b) its corresponding SAED pattern, (c) high-magnification TEM image, and (d) FE-SEM image

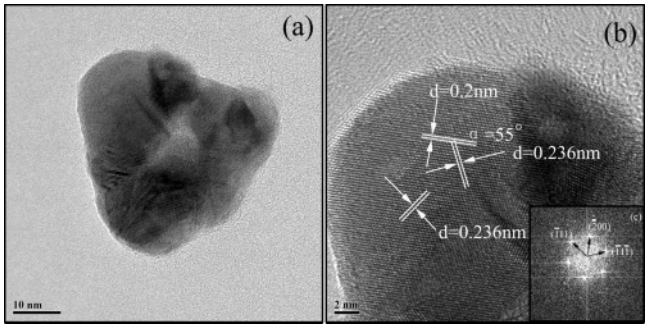

Figure 3. Single Ag nanoshell selected to be undertaken for HRTEM observation: (a) morphology micrograph, (b) HRTEM image, and (c) its corresponding FFT pattern.

2b, the angle between the two stripes is 55°. Combined with its corresponding FFT pattern (Figure 3c and the insert in Figure 3b), these planes can be indexed to (−200), (−111), and ($-11\bar{1}$) of fcc Ag.

In the present work, citric acid served as a capping agent to prevent the growth of Co nanoparticles through repulsive forces between negatively charged cobalt nanoparticles, which had the same use in preventing the resulting Ag nanoshells from aggregating. Using $NaBH_4$ as a reducing agent has two advantages. First, the strong reduction ability can reduce Co^{2+} rapidly, which presents a rapid nucleation condition for forming small-sized metal nanoparticles; second, superfluous $NaBH_4$ in the system will not interfere with the latter replacement reaction between Co and Ag^+, because $NaBH_4$ can be consumed by the reaction with water. Most other reducing agents cannot meet these requirements. Scheme 1 shows the sketch map of the formation mechanism of Ag nanoshells. Because of the strong reaction driving force resulting from the difference in reduction potential between the Ag^+/Ag and Co^{2+}/Co redox couples, the replacement reaction occurred immediately when $AgNO_3$ was introduced

Scheme 1. Sketch Map of the Formation Mechanism of the Ag Nanoshell

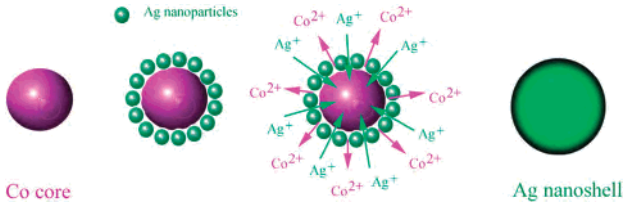

into the Co nanoparticle suspension and formed a thin Ag film on the surface of the Co nanoparticles. As the reaction continued, Co^{2+} and Ag^+ continuously diffused through the film until the Co cores were completely consumed and a hollow Ag nanoshell was formed. Yin et al. [26] have proposed a strategy for constructing hollow nanocrystals through the nanoscale Kirkendall effect, in which pores form because of the difference in diffusion rates between two components in a diffusion couple. In the present work, the formation of Ag nanoshells can also be attributed to a similar Kirkendall effect, which can explain why the products are hollow nanoshells but not solid nanoparticles. At the interface of Ag and Co, the diffusion rate of atomic Co is much faster than that of atomic Ag, which results in a net directional flow of matter outward. The outward-diffused Co atom will be oxidized into Co^{2+} by Ag^+ at once. So the cavities with sizes similar to the sizes of Co nanoparticles are kept after the Co cores are consumed thoroughly. Because of the small size of Co cores, both the outer and inner diameters of the as-prepared Ag nanoshell are in the nanometer scale.

To prove this assumption, we carried out a series of comparative experiments, which was similar to the process used to prepare Ag nanoshells except for some modifications. First, $AgNO_3$ was not directly introduced to the newly formed Co nanoparticle suspension, but the as-prepared Co nanoparticles were separated and washed by centrifugation repeatedly before being introduced to $AgNO_3$ solution instead. So, the reaction between Co and $AgNO_3$ occurred immediately. The as-prepared sample was marked as sample I, whose TEM micrographs are shown in panels a and b of Figure 4. The low-magnification TEM image shown in Figure 4a indicates that the products are composed of nanospheres and nanoshells. In the high-magnification TEM image shown in Figure 4b, a special yolk−shell nanostructure inspires us to speculate that this structure resulted from incomplete replacement reaction between Co and $AgNO_3$. Using EDS microprobe analysis, we can clearly prove the element composition. Panels a and b of Figure 5 show the EDS patterns of Ag nanoshells and Co−Ag yolk−shell nanostructure, respectively. In Figure 5a, the EDS pattern corresponds to the samples shown in Figure 2, indicating that except for the peaks of C and Cu, which come from the Cu grid, the peak of Ag is the only signal from the product. There is no signal from Co, which indicates that the cobalt nanoparticles have been depleted thoroughly during the process. However, the EDS pattern in Figure 5b, which corresponds to the yolk−shell nanostructure, clearly shows

(26) Yin, Y. D.; Rioux, R. M.; Erdonmez, C. K.; Hughes, S.; Somorjai, G. A.; Alivisatos, A. P. *Science* **2004**, *304*, 711.

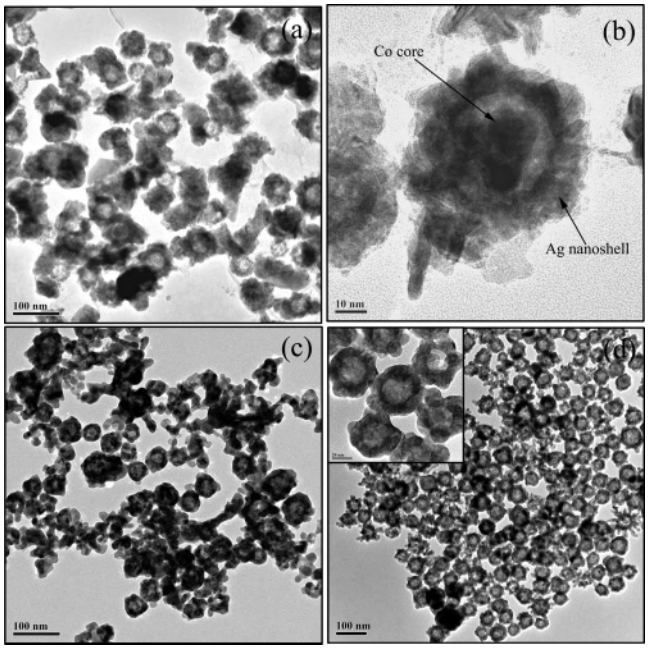

Figure 4. TEM images of the Ag samples prepared in the comparative experiments: (a,b) sample I, nanoshells and yolk−shell nanostructure; (c) sample II, nanoparticles and nanoshells; (d) sample III, nanoshells.

a Co signal, indicating the presence of the Co core. In fact, this yolk−shell nanostructure is the intermediate product, which has a tendency to grow into a hollow Ag nanoshell with continuing provision of Ag^+. But why is the reaction incomplete? It may be the relative low reaction activity compared to that of the newly formed Co nanoparticles in the in situ replacement reaction. This phenomenon was also found in the reported preparation of Ni@Ag and Co@Ag core−shell nanostructures, [18,21] in which the surfactant sustained the reaction at the interfaces.

Second, if the $AgNO_3$ was introduced into a Co nanoparticle suspension as soon as the Co nanoparticles were formed by the reduction of $NaBH_4$, the products took on a different morphology. The as-prepared sample was marked as sample II, whose TEM morphology is shown in Figure 4c, which indicates that the products are composed of lots of nanoparticles and a small quantity of nanoshell. Because at this stage large quantities of Ag^+ ions were reduced directly by $NaBH_4$, only part of the Ag^+ ions reacted with the newly formed Co nanoparticles. It is obvious that these quantities of nanoparticles result from the reduction of $NaBH_4$. In fact, because citric acid was selected as the capping agent, the whole solution was a weak acid containing H^+ and NO_3^-. So the reaction solution system had a strong oxidation ability and the newly formed tender Co nanoparticles were easily dissolved again. In the whole procedure, we found that after being magnetically stirred beyond 30 min, the deep brown Co nanoparticle suspension turns colorless. We wondered why the core of Co nanoparticles was dissolved by the solution but not by the reaction between Ag^+ ions and Co nanoparticles; we carried out the third comparative experiment, in which the capping agent was replaced by trisodium citrate while the other conditions were unchanged. The as-prepared sample was marked as sample III, whose TEM images are shown in Figure 4d. The TEM micrograph shows the product is composed of well-dispersed nanoshells with outer diameters of 40−60 nm and a wall thickness of ∼10 nm. The high-magnification TEM image inserted in Figure 4a shows further details that the cavities of these nanoshells are smooth, although the outer surfaces are so irregular; this indicates an advancing trace of the interface during the replacement reaction. The above comparative experiments well-confirm the assumption of the formation mechanism for Ag nanoshells.

In another comparative experiment, Ag nanoparticles were prepared through direct reduction of $AgNO_3$ by $NaBH_4$, also using citric acid as the stabilization agent. TEM observation indicates a particle size of ∼20 nm (not shown). The UV−vis absorption spectra of Ag nanoshells and nanoparticles are shown in Figure 6, which shows that the shape and structure have great effect on the position and shape of the absorption peak. The nanoparticles have a plasmon peak at 395 nm and a weak shoulder peak around 350 nm. The case of the nanoshells is quite different, with a plasmon peak that has red-shifted to 506 nm. Metal nanoshells with shell layers consisting of metals with strong plasmon resonances exhibit a strong, plasmon-derived optical resonance, typically shifted to much longer wavelengths than the plasmon resonance of the corresponding solid metal nanosphere.[3,27] The above spectral results, in combination with the TEM images, strongly indicate the as-prepared nanostructure is indeed a nanoshell with a hollow interior. Furthermore, there is still a wide absorption in the visible region beyond 600 nm, which

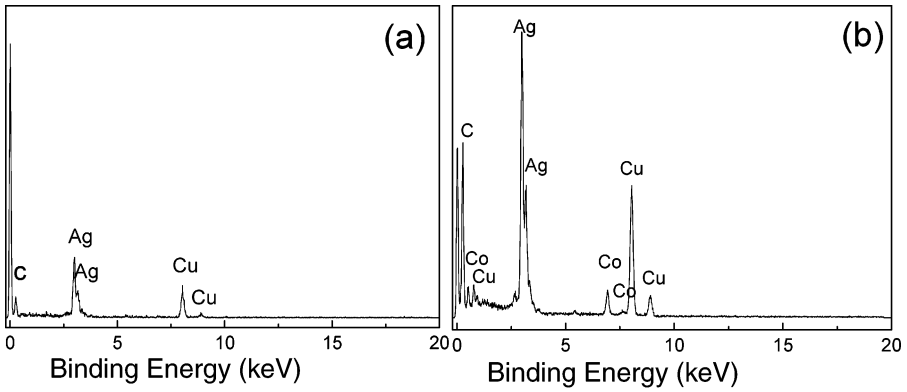

Figure 5. EDS patterns of the as-prepared Ag nanoshells and Co−Ag yolk−shell nanostructure.

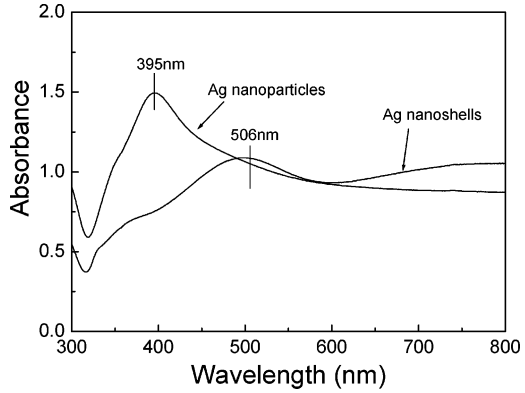

Figure 6. UV−vis absorption spectra of the as-prepared Ag nanoshells and nanoparticles.

is similar to the reported results by Halas and co-workers,[27] who also revealed that the plasmon peak of nanoshells could be conveniently tuned from the visible region to the far-infrared region through controlling the wall thickness and core diameter. This interesting property makes these Ag nanoshells good candidates for application in photothermal biomaterials, such as photothermally triggered drug release, photothermal cancer therapy, and contrast-enhanced imaging.

Conclusion

In summary, Ag nanoshells with outer diameters of 40−50 nm and inner diameters of 20−30 nm were successfully synthesized by a facile in situ replacement reaction using Co nanoparticles as sacrificial templates, which can be easily enlarged to the gram scale. The reaction driving force comes from the large reduction potential gap between the Ag^{+}/Ag and Co^{2+}/Co redox couples, which results in the consumption of Co cores and the formation of a hollow cavity of Ag nanoshells. The UV−vis spectrum of this nanostructure exhibits a distinct difference from that of solid nanoparticles.

IC060539J

(27) Jackson, J. B.; Halas, N. J. *J. Phys. Chem. B* **2001**, *105*, 2743.